

# AN ACCURATE EXPRESSION FOR THE INPUT IMPEDANCES OF ONE-SIDED MICROSTRIP PROBES IN WAVEGUIDE

S. Withington, G. Yassin, J. Leech, and K.G. Isaak

*Department of Physics,  
University of Cambridge,  
Madingley Rd, Cambridge.*

## Abstract

In previous work we established a general procedure for calculating the input impedances of one-sided microstrip probes in waveguide. The *one-sided* configuration, where the probe extends only part way across the waveguide, contrasts with the *two-sided* configuration, where the probe extends the whole way across the waveguide. We demonstrated that because of the way in which the different current distributions couple to the waveguide modes, the one-sided probe is intrinsically lower impedance and more broadband than the two-sided probe. This observation has important consequences for the design of THz SIS waveguide mixers.

Previously, we had to make an approximation when evaluating the integral for the complex radiated power, and this led to a corresponding approximation in the final expression for the input impedance. We have now evaluated this integral rigorously, and we have shown that the original approximation breaks down to third order in the width of the probe, an effect we have seen experimentally. In this paper, we review the technique for calculating the impedances of one-sided microstrip probes, and we present a more accurate expression based on a rigorous analytical evaluation of the power integral. This expression is compared with complex impedances measured on a scale model at 5GHz, and excellent agreement is found.

## 1 Introduction

The planar waveguide probe has become the standard way of coupling SIS tunnel junctions to rectangular waveguides in conventional low-noise submillimetre-wave mixers. In the most popular configuration, the tunnel junction is placed at the centre of a thin conducting strip that extends the whole of the way across the waveguide [1]. This arrangement has the disadvantage that it is not possible to obtain low values of input impedance ( $50 \Omega$  or less) without reducing the height of the waveguide. This property is intrinsic to the “two-sided” geometry, and is a consequence of the fact that the contributions from the evanescent waveguide modes add up in parallel and influence the real part of the input impedance in an complicated way. An alternative approach is to use a metallisation that extends only part way across the waveguide: a “one-sided” probe. In this case, the contributions from the waveguide modes add up in series, and only the propagating fundamental mode couples to the resistive part of the input impedance. As a consequence, the input impedance is low,

and does not exhibit the complicated frequency dependence of the two-sided arrangement. The ease with which it is possible to couple low-impedance devices to one-sided probes in full height waveguide has important consequences for the design of THz SIS mixers.

In a previous paper [2], we established a general procedure for calculating the input impedances of one-sided microstrip probes in waveguide. The approach was based on the reciprocity theorem and the spectral-domain method [3]. The main feature of the theory is that the Fourier transforms of the current and field distributions are related—through the spectral dyadic Green's function—by an algebraic rather than an integral equation. Moreover, the expression for the spectral Green's function is much simpler and easier to obtain than the space-domain version—especially for dielectrically-loaded waveguide. Originally, we had to make an approximation when evaluating the integral for the complex radiated power, and this led to a corresponding approximation in the expression for the input impedance. We have now evaluated this integral rigorously and have shown that the original approximation was accurate to only second order in the width of the probe. Indeed, the original expression was accurate for narrow probes only, an effect we had seen experimentally.

In this paper, we present an accurate expression for the input impedance of one-sided microstrip probes. The expression is based on a rigorous analytical evaluation of the power integral. The physical significance of the various terms in the final expression is clear. Through this work we have found that a broadband match can be achieved by using a radial probe. We describe how, by using the Fast Fourier Transform, the basic technique can be extended to cover any geometry for which the current distribution is approximately known.

## 2 Theoretical Analysis

In Fig. 1, we show the geometry of a microstrip probe in waveguide. The probe is assumed to be fed by a current source  $I_{in}$ , which is connected between the base of the probe and the wall of the waveguide. This source causes a potential difference  $V_{ab}$  to be established, through which the input impedance can be defined:

$$Z_{in} = \frac{V_{ab}}{I_{in}} . \quad (1)$$

Using the reciprocity theorem [4],[5], we can derive an expression for  $V_{ab}$  in terms of the current density on the surface of the probe  $J_x$  and the tangential electric field in the waveguide  $E_x$ ; in this way, we obtain

$$Z_{in} = -\frac{1}{I_{in}^2} \int \int \int E_x(r) J_x(r) dV . \quad (2)$$

When evaluating the above integral we assume that the current is distributed sinusoidally over the length of the probe. This assumption allows a great deal of simplification and eventually leads to a closed-form solution for the input impedance. All of our detailed experimental measurements show that this first-order guess at the current distribution gives extremely accurate results. We therefore write

$$J_x(x, y, z) = J_0 \delta(y - d) u(z) \sin k(x_1 - x) \quad (3)$$

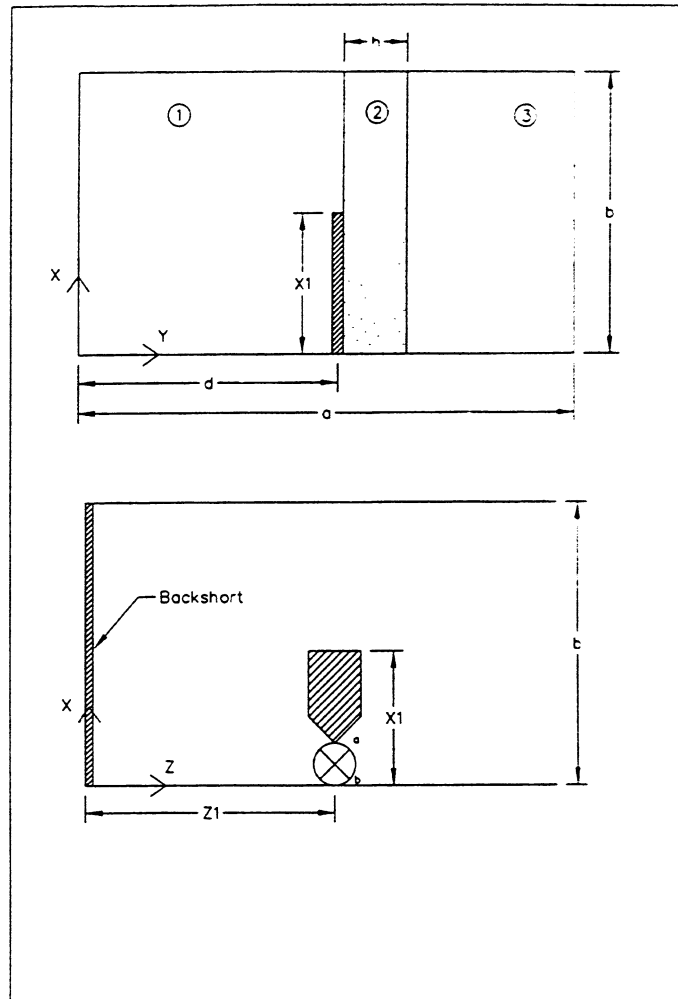


Figure 1: A one-sided microstrip probe in waveguide

for  $x < x_1$  and zero otherwise.  $u(z)$  describes the current density distribution across the width of the probe. Previously, we used an expression of the form

$$u(z) = \frac{1}{\pi} \frac{1}{\sqrt{1 - \left(\frac{z-z_1}{w}\right)^2}} \quad |z - z_1| < w, \quad (4)$$

where  $w$  is the half width of the probe, to take into account the singularity that exists, in the case of infinitely thin metallisation, at the edge of the strip. In this paper, we simply assume that the current is constant across the width of the strip and goes to zero at the edges:  $u(z) = 1$  for  $|z - z_1| < w$  and zero otherwise. For all practical purposes, these two current distributions are identical. Notice that we are assuming that the plane of the probe lies in the E-plane of the waveguide. In a previous paper we proved analytically that the input impedance is insensitive to the orientation of the probe. In the following treatment, we shall neglect the transverse components of the current  $J_z$  and the electric field  $E_z$ . Rigorous theoretical analyses of microstrip lines suggest strongly that this approximation, which significantly simplifies the solution, is a good one for geometries of practical interest.

To apply the spectral-domain method to our problem, we first replace the current and field in (2) by their Fourier transforms and apply Parseval's theorem in two dimensions to obtain

$$Z_{in} = -\frac{1}{8\pi b} \frac{1}{I_{in}^2} \sum_{n=-\infty}^{+\infty} \int_{-\infty}^{+\infty} \tilde{E}_x(\alpha_n, \beta, d) \tilde{K}_x^*(\alpha_n, \beta) d\beta, \quad (5)$$

where  $\tilde{K}_x(\alpha_n, \beta)$  is the two-dimensional Fourier transform of the current distribution. At this stage, the boundary conditions at the top and bottom of the waveguide have effectively been introduced by the method of images: forcing the Fourier parameter  $\alpha$  to be discrete.

The input impedance can now be calculated by using the spectral-domain relationship between the current and field distributions. Neglecting the transverse component of the field and current we obtain

$$\tilde{E}_x(\alpha_n, \beta, d) = \tilde{G}_{xx}(\alpha_n, \beta, d) \cdot \tilde{K}_x(\alpha_n, \beta) \quad (6)$$

where

$$\tilde{G}_{xx}(\alpha, \beta, d) = \frac{\alpha^2}{\alpha^2 + \beta^2} Z^e + \frac{\beta^2}{\alpha^2 + \beta^2} Z^h. \quad (7)$$

In the above equations  $\tilde{G}_{xx}(\alpha, \beta, d)$  is the longitudinal component of the dyadic Green's function, evaluated at  $d$ .  $Z^e$  and  $Z^h$  are the Green's functions associated with the LSE and LSM modes and expressions for them may be found in several places [6]. We can, if desired, take into account the effect of the supporting dielectric substrate simply by using the appropriate Green's function.

Substitution then gives

$$Z_{in} = -\frac{1}{4\pi b} \frac{1}{I_{in}^2} \sum_{n=-\infty}^{+\infty} \int_{-\infty}^{+\infty} \tilde{G}(\alpha_n, \beta, d) \left| \tilde{K}_x(\alpha_n, \beta) \right|^2 d\beta, \quad (8)$$

where for convenience we have dropped the subscript on the Green's function.

To proceed with the analysis, we need the spectral domain dyadic Green's function for an empty waveguide and the Fourier transform of the current distribution. To derive an expression for the Fourier-transformed current distribution we can use the method of

images; that is to say we replaced the wall of the waveguide by a virtual probe. The virtual probe is identical to the actual probe, but points in the opposite direction. We then find,

$$\bar{K}_x(\alpha_n, \beta) = I_{in} \frac{2k}{(k^2 - \alpha_n^2)} \left[ \frac{\cos \alpha_n x_1 - \cos k x_1}{\sin k x_1} \right] \left[ \frac{\sin \beta w}{\beta w} \right], \quad (9)$$

where boundary conditions require

$$\alpha_n = \frac{n\pi}{b}. \quad (10)$$

Substituting the current distribution into the expression for the impedance we find

$$Z_{in} = \frac{-1}{2\pi b} \sum_{n=0}^{+\infty} \delta_n \frac{k^2}{(k^2 - \alpha_n^2)^2} \left[ \frac{(\cos \alpha_n x_1 - \cos k x_1)}{\sin k x_1} \right]^2 \int_{-\infty}^{+\infty} \tilde{G}(\alpha_n, \beta, d) \left[ \frac{\sin \beta w}{\beta w} \right]^2 d\beta, \quad (11)$$

$$\text{and } \delta_n = \begin{cases} 1 & \text{for } n=0 \\ 2 & \text{otherwise} \end{cases}.$$

To make further progress we need an expression for the spectral Green's function of empty waveguide. Using the immittance method, and assuming that the probe is at the centre of the waveguide, we find

$$\tilde{G}(\alpha_n, \beta, d) = \frac{jkR_0}{2\gamma} \left[ \frac{k^2 - \alpha_n^2}{k^2} \right] \tanh \gamma d, \quad (12)$$

where  $R_0$  is the impedance of free space, and  $\gamma$  is the propagation constant in the transverse direction.

Substituting the expression and using an expansion for the hyperbolic tangent, we arrive at

$$Z_{in} = \frac{-jkR_0}{\pi ab} \sum_{n=0}^{+\infty} \sum_{m=1}^{+\infty} \delta_n \frac{1}{(k^2 - \alpha_n^2)} \left[ \frac{(\cos \alpha_n x_1 - \cos k x_1)}{\sin k x_1} \right]^2 \sin^2 \left( \frac{m\pi}{2} \right) \int_{-\infty}^{+\infty} \frac{1}{(\beta^2 - \beta_{mn}^2)} \left[ \frac{\sin \beta w}{\beta w} \right]^2 d\beta. \quad (13)$$

In the above equation,  $\beta_{mn}$  are the poles of  $\tilde{G}$  which satisfy the relation

$$\beta_{mn}^2 = k^2 - \gamma_m^2 - \alpha_n^2 \quad (14)$$

where the propagation constant in the transverse direction is given by

$$\gamma_m = \left( \frac{m\pi}{a} \right). \quad (15)$$

For functions of this kind the value of the integral is determined by the poles of the integrand. In the case of propagating modes, the  $\beta_{mn}$  are real, and the poles lie on the real axis of the complex plane and contribute to the real part of the input impedance through the singularities that exist when integrating along the real line from  $-\infty$  to  $+\infty$ . In the case of non-propagating modes, the poles lie on the imaginary line and contribute to the reactive part of the input impedance—they do not produce singularities on the real line. Hence, we

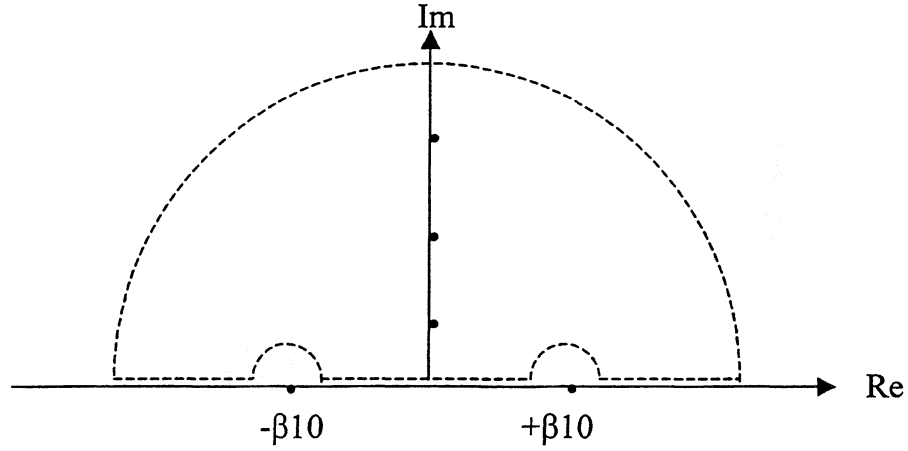


Figure 2: Poles of the power radiation integral in the complex plane. The poles on the real line correspond to the propagating modes, and the poles on the imaginary line correspond to the evanescent modes.

should perform the integrals for the propagating and none propagating modes separately. For convenience, we shall assume that the size of the waveguide has been chosen so that only the lowest-order mode can propagate. In this case, only  $\beta_{10}$  is real. The situation is shown in Fig. 2.

We can now use the residue theorem easily to get the input resistance of a free-standing one-sided microstrip probe in waveguide:

$$R_{in} = \frac{R_0}{abk\beta_{10}} \tan^2 \left[ \frac{kx_1}{2} \right] \left[ \frac{\sin \beta_{10}w}{\beta_{10}w} \right]^2. \quad (16)$$

This expression is identical to our early one apart from the appearance of a sinc-squared function rather than a Bessel function due to the different assumption about the transverse current distribution.

In the case of the imaginary part, the integral in (14) becomes

$$X_{in} = \frac{kR_0}{ab} \left[ \sum_{m=2}^{+\infty} X_{m0} + \sum_{n=1}^{+\infty} \sum_{m=1}^{+\infty} X_{mn} \right] \quad (17)$$

$$X_{mn} = \delta_n \frac{1}{(k^2 - \alpha_n^2)} \frac{1}{\beta_{mn}} \left[ \frac{\cos \alpha_n x_1 - \cos kx_1}{\sin kx_1} \right]^2 \sin^2 \left( \frac{m\pi}{2} \right) \left[ \frac{2\beta_{mn}w - 1 + \exp^{-2\beta_{mn}w}}{2(\beta_{mn}w)^2} \right]. \quad (18)$$

This equation is similar to the approximate expression for the reactive part of the input impedance derived previously. Now, however, the sinc-squared function in  $\beta_{mn}w$  is replaced by the last term in square brackets of (23). For all real probes  $\beta_{mn}w$  is less than unity.

Expanding the sinc-squared function and the exponential function as power series and comparing the two, we find that the third-order term in our original expression is incorrect; an effect which we see experimentally when the width of the probe becomes large.

Clearly, the propagating mode does not make a contribution to the reactive part of the input impedance. Also it can be seen that the contributions of the different modes to the overall reactance change sign depending on whether or not  $k > \alpha_n$ . In fact the contributions are inductive for  $n = 0$  and capacitive for  $n > 0$ . Hence, the overall input impedance can be inductive or capacitive depending on the height of the waveguide and the frequency.

Finally, we would like to include the effect of a backshort in the analysis. There are various ways in which this can be achieved. To a good approximation we can simply multiply the Green's function associated with the unterminated waveguide by the factor

$$\tau = 2j \sin \beta z_1 \exp -j\beta z_1 , \quad (19)$$

where  $z_1$  is the distance between the centre of the probe and the backshort. In addition, we only include this factor in the integration over  $\beta$  when considering the propagating mode, and we ignore the effect on the non-propagating modes. This assumption makes the integral easy to evaluate and has physical justification because the backshort is usually sufficiently far from the probe that the near-field effects of the non-propagating modes are negligible. It is the reactive contribution of the lowest-order mode that can be used to cancel the reactive effects of the non-propagating modes in order to tune the probe for any frequency.

Finally, the input impedance,  $Z_{in} = R_{in} + jX_{in}$ , of a free-standing centred, one-sided probe with backshort is given by

$$R_{in} = \frac{2R_0}{abk\beta_{10}} \tan^2 \left[ \frac{kx_1}{2} \right] \left[ \frac{\sin \beta_{10}w}{\beta_{10}w} \right]^2 \sin^2 (\beta_{10}z_1) \quad (20)$$

$$X_{in} = X_{10} + \frac{kR_0}{ab} \left[ \sum_{m=2}^{+\infty} X_{m0} + \sum_{n=1}^{+\infty} \sum_{m=1}^{+\infty} X_{mn} \right] \quad (21)$$

$$X_{10} = \frac{R_0}{abk\beta_{10}} \tan^2 \left[ \frac{kx_1}{2} \right] \left[ \frac{\sin \beta_{10}w}{\beta_{10}w} \right]^2 \sin (2\beta_{10}z_1) \quad (22)$$

$$X_{mn} = \delta_n \frac{1}{(k^2 - \alpha_n^2)} \frac{1}{\beta_{mn}} \left[ \frac{\cos \alpha_n x_1 - \cos kx_1}{\sin kx_1} \right]^2 \sin^2 \left( \frac{m\pi}{2} \right) \left[ \frac{2\beta_{mn}w - 1 + \exp^{-2\beta_{mn}w}}{2(\beta_{mn}w)^2} \right] . \quad (23)$$

In all of these equations  $\beta_{mn}$  corresponds to  $|\beta_{mn}|$ , that is to say we use the modulus of the propagation constant regardless of whether the mode is propagating or not.

In general, we see that for the microstrip probe the real part of the input impedance is due solely to the lowest-order propagating mode; whereas for the two-sided probe, the real part of the input impedance is influenced by a large number of high-order non-propagating modes. This basic and important difference results in the one-sided probe being characterised by a high value of input impedance whereas the microstrip probe is characterized by a relatively low value of input impedance. In order to reduce the input impedance of the two-sided probe, and also to increase the bandwidth, the height of the waveguide is usually reduced by a factor of about 4, but this modification increases the conduction losses

and the manufacturing complexity—both of which are extremely important if one wants to manufacture components for the THz frequency range.

### 3 Experimental Results and Discussion

To investigate the above theory, we manufactured a scale model of a 400-500GHz mixer block. The waveguide had dimensions of  $a=47\text{mm}$  and  $b=22\text{mm}$ , and the probe was fed by an SMA connector which was inserted into the centre, ( $d = a/2$ ), of the broad wall. The central conductor of the SMA connector penetrated 0.5mm into the waveguide and a copper-foil probe was soldered to the end. A major advantage of this arrangement is that a short circuit can be applied at the wall of the waveguide in order to establish a well-defined reference plane for the impedance measurements. It is substantially more difficult to do well-calibrated impedance measurements on a two-sided probe. In order to separate out the intrinsic behaviour of the probe from the behaviour of the probe-backshort combination, we performed measurements on a waveguide that was terminated by two matched loads. The real and imaginary parts of the input impedance were then measured by using a Vector Network Analyser.

In Fig. 3 we show the input impedance of a doubly-matched probe as a function of frequency. In this case the probe was 3mm wide,  $2w$ . As can be seen, the measurements are in excellent agreement with the theory over the whole range of frequencies tested. An important observation is that the microstrip probe is essentially a low-impedance structure with a typical input resistance in the range 10-100 $\Omega$ . This range is ideally suited to the characteristic impedances of microstrip lines. From the point of view of SIS mixers, the probe can be used for feeding SIS tunnel junctions over broad ranges of frequency without the need to reduce the height of the waveguide.

We also notice in Fig. 3 that the agreement between theory and experiment is extremely good apart from the resistive component of the longest probe. In fact, as the length of the probe was increased further, so that it became significantly longer than half of the waveguide height, the agreement between theory and experiment deteriorated even more. We attribute the inability of our theory to predict the behavior of very long probes as being due to the fact that the assumption of a one-term sinusoidal current distribution along the length of the probe breaks down.

Because the derivation of the analytical result is rather involved, we have checked the result by evaluating the integral in (11) numerically after substituting the expression for the Green's function given by (12). This reactance has also been plotted in Fig. 3. Clearly, the two are in agreement showing the integrity of our analytical expressions.

Overall, the above result shows that whereas the two-sided probe is essentially a high-impedance structure, the one-sided probe is a low-impedance structure. Moreover, wideband operation can be obtained with a one-sided probe without the need to reduce the height of the waveguide. In fact, wideband operation with low impedance levels can be obtained with *increased-height* waveguide, and this implies that the upper frequency limit to which waveguide mixers can be manufactured can be extended well into the THz frequency range.

Because of the intrinsic advantages of the one-sided probe, we have started to look at other shapes of metallisation. Shown in Fig. 4 is the input return loss of a radial probe on a quartz substrate. The scale model had a waveguide size of  $22\times 47\text{mm}$ , a radius of 9mm, and a quartz substrate measuring  $7\times 12.5\text{mm}$ . The probe had an opening angle of  $90^\circ$ , and the



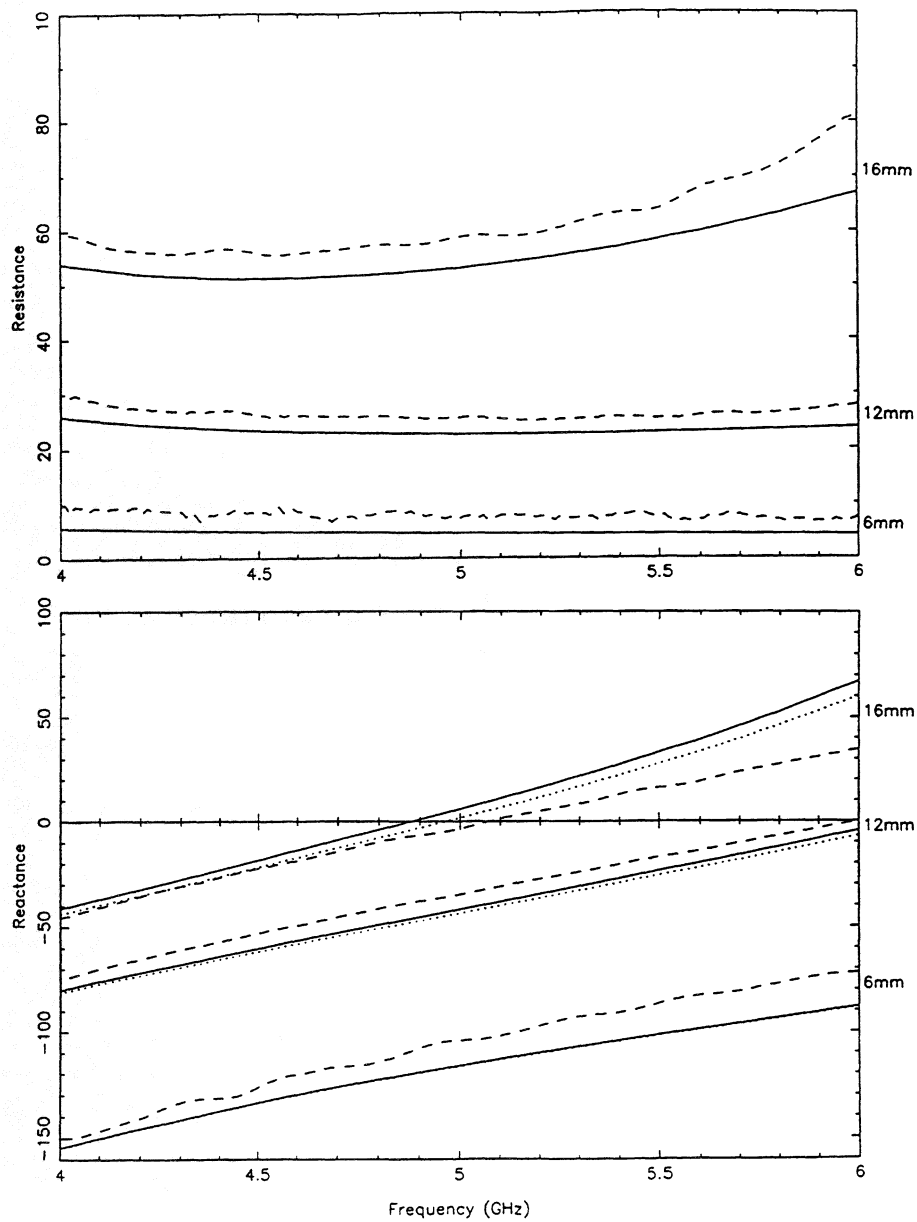


Figure 3: The input impedance of a doubly-matched microstrip probe as a function of frequency for  $2w = 3\text{mm}$ . The waveguide measured  $47\text{mm} \times 22\text{mm}$ , and the probe was in the centre of the waveguide. The dashed lines correspond to the experimental data, the dotted lines to the numerical integration, and the solid lines to the analytical expressions.

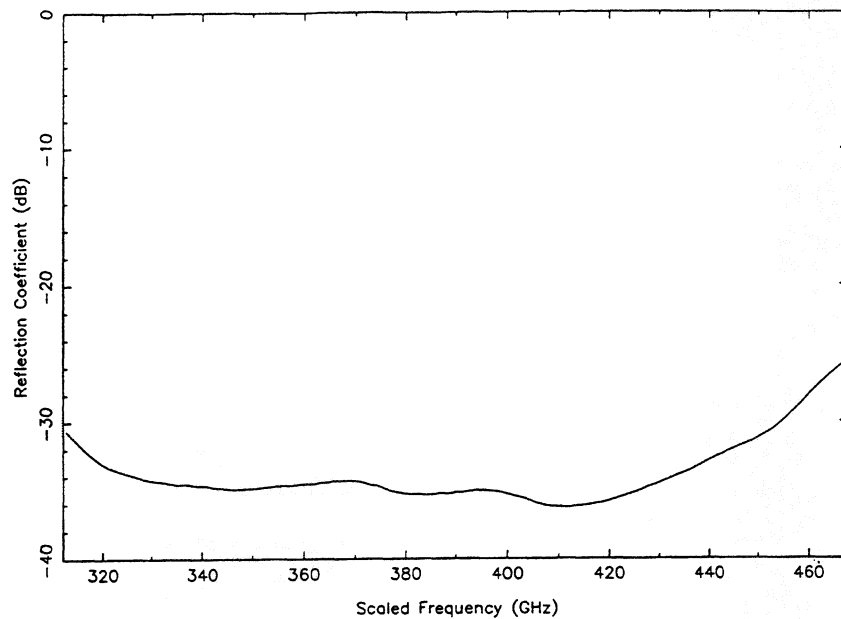


Figure 4: The input reflection coefficient, normalised to  $30\Omega$ , of the radial probe described in the text. The frequency scale is that of the final device rather than the model.

backshort was at a distance of 10mm relative to the centre of the probe. This type of probe has the remarkable property that its input impedance is purely real over a very wide range of frequencies, and the resistance is low and can be adjusted merely by changing the length of the probe. In order to investigate this design, and also the hammer-head arrangement used by Kerr [7], theoretically, we have generalised our procedure to handle more complicated current distributions. This has been achieved by evaluating the integral in (8) numerically after calculating the current distribution by means of a Fast Fourier Transform. The results for the rectangular probe described above are the same as the analytical expression derived here, and we are now employing this method to study more complicated geometries.

## 4 Conclusions

We have derived an analytical expression for the input impedances of one-sided microstrip probes in waveguide, where the integral for the complex radiated power has been evaluated rigorously. We find that, compared to our previous work, where an approximation was made, there is a small difference in the expression for the reactive contributions of the evanescent waveguide modes. The error is, however, only third order in  $\beta_{mn}w$ , where  $\beta_{mn}$  is the modulus of the propagation constant and  $w$  the half-width of the probe.

We conclude that combined with our previous work, we have a rigorous way of calculating the input impedances of one-sided microstrip probes. The supporting dielectric substrate can be taken into account by using the appropriate Green's function. It is important to include the effect of the substrate in submillimetre-wave components, where the substrate

can occupy a significant fraction of the waveguide.

By using a procedure based on the Fast Fourier Transform, we are now extending our analysis to cover other probe geometries, and other current distributions, such as that of the radial probe.

## References

- [1] R.L. Eisenhart and P.J. Khan, "Theoretical and experimental analysis of a waveguide mounting structure," *IEEE Trans. Microwave Theory Tech.*, vol. MTT-19, pp. 706-717, 1971.
- [2] G. Yassin and S. Withington, "Analytical Expression for the Input Impedance of a Microstrip Probe in Waveguide," *Int. J. Infrared and Millimetre Waves*, vol. 17, pp.1685-1705, 1996.
- [3] T.Q. Ho and Yi-Chi Shih, "Spectral-domain analysis of E-plane waveguide to microstrip transition," *IEEE Trans. Microwave Theory Tech.*, vol. MTT-37, pp. 388-392, 1989.
- [4] W.L. Weeks, *Electromagnetic Theory for Engineering Applications*, John Wiley & Sons, Inc.: New York, 1964.
- [5] V.H. Rumsey "Reaction concept in electromagnetic theory," *Phys. Rev.*, vol. 94, pp. 1483-1491, 1954.
- [6] Q. Zhang and T. Itoh, "Spectral-domain analysis of scattering from E-plane circuit elements," *IEEE Trans. Microwave Theory Tech.*, vol. MTT-35, pp. 138-150, 1987.
- [7] A.R. Kerr and S.-K. Pan, "Some recent developments in the design of SIS mixers," *Int J. Infrared Millimetre Waves*, vol. 11, pp. 1169-1187, 1990.